PUBLISHED VERSION

Maria Caruso, Kim Y.C. Fung, James Moore, Gemma V. Brierley, Leah J. Cosgrove, Michelle Thomas, Glenice Cheetham, Emma Brook, Louise M. Fraser, Teresa Tin, Ha Tran, Andrew Ruszkiewicz
Claudin-1 expression is elevated in colorectal cancer precursor lesions harboring the BRAF V600E mutation

http://hdl.handle.net/2440/90938

Claudin-1 Expression Is Elevated in Colorectal Cancer Precursor Lesions Harboring the BRAF V600E Mutation[1,2]

Maria Caruso[*], Kim Y.C. Fung[†], James Moore[‡,¶],
Gemma V. Brierley[†], Leah J. Cosgrove[†],
Michelle Thomas[‡,¶], Glenice Cheetham[§],
Emma Brook[¶], Louise M. Fraser[¶], Teresa Tin[*],
Ha Tran[*] and Andrew Ruszkiewicz[*,¶,#]

[*]Centre for Cancer Biology, Gastroenterology Research Laboratory, University of South Australia, Adelaide, Australia; [†]CSIRO Preventative Health National Research Flagship, Adelaide, Australia; [‡]Royal Adelaide Hospital, Adelaide, Australia; [§]Molecular Pathology, SA Pathology, Adelaide, Australia; [¶]University of Adelaide, Adelaide, Australia; [#]Genetic Pathology, SA Pathology, Adelaide, Australia

Abstract

BACKGROUND: Sessile serrated adenomas/polyps (SSA/P) are now recognised precursors of colorectal cancer (CRC) including cancers harbouring somatic BRAF (V600E) mutations. While the morphological diagnostic criteria of SSA/P have been established, distinguishing between small/early SSA/P and microvesicular hyperplastic polyps (MVHP) is challenging and may not be possible in routine practice. METHODS: Gene expression profiling of MVHP ($n=5$, all BRAF V600E wild-type) and SSA/P ($n=5$, all BRAF V600E mutant) samples was performed. Quantitative reverse transcription–polymerase chain reaction (qRT-PCR) and immunohistochemical analysis was performed to verify the expression of claudin 1 (CLDN1) in MVHP and SSA/P. RESULTS: Gene expression profiling studies conducted between MVHP and SSA/P identified CLDN1 as the most statistically significant differentially expressed gene ($p<0.05$). Validation with qRT-PCR confirmed an up-regulation of CLDN1 in BRAF V600E mutant polyps regardless of polyp type ($p<0.0005$). Immunohistochemical analysis of CLDN1 expression in BRAF V600E mutant SSA/Ps ($n=53$) and MVHPs ($n=111$) and BRAF wild-type MVHPs ($n=58$), demonstrated a strong correlation between CLDN1 expression and the BRAF V600E mutation in both SSA/P and MVHP samples when compared to wild-type polyps ($p<0.0001$). CONCLUSION: This study demonstrates an up regulation of CLDN1 protein in serrated colorectal polyps including MVHP harbouring the BRAF V600E mutation. Our results demonstrated an apparent heterogeneity on the molecular level within the MVHP group and suggest that MVHP with somatic BRAF V600E mutation and up-regulated expression of CLDN1 are closely related to SSA/P and may in fact represent a continuous spectrum of the same neoplastic process within the serrated pathway of colorectal carcinogenesis.

Introduction

While the majority of colorectal cancer (CRC) is believed to evolve through the conventional adenoma to carcinoma sequence, initially proposed by Vogelstein [1], it has become apparent that as many as 30% of CRCs may arise through an alternate route, known as the serrated pathway [2]. The sessile serrated adenoma/polyp (SSA/P) has been recently accepted as the most common precursor lesion for this pathway and its correct identification in clinical and pathologic practice is of critical importance. Currently, pathologic diagnosis of SSA/P is based on a constellation of cytoarchitectural histopathologic features including the degree of crypt dilation and serration, the horizontal crypt configuration, number of branched crypts and nuclear features [3,4]. However, SSA/Ps, particularly when small, have overlapping microscopic features with other serrated polyps, including microvesicular hyperplastic polyps (MVHP), and distinction between these lesions may not always be possible in routine pathology practice. On a molecular level, the serrated pathway is characterized by the *V600E* somatic mutation in the BRAF proto-oncogene *(BRAF V600E)*, cytosine guanine dinucleotide island methylator phenotype (CIMP), and microsatellite instability (MSI) [4,5]. The *BRAF V600E* mutation is hypothesized to be an early event in this pathway that potentially drives tumorigenesis [5], whereas in the conventional pathway, mutations in the *adenomatous polyposis coli* gene and aberrant Wnt signaling are widely accepted as initiating events [6].

Despite the growing data on molecular features of the serrated pathway, our understanding of the key biologic events involved in the development of polyps in this pathway and their progression to carcinoma is still not complete. Molecular studies including gene expression profiling comparing different subsets of CRC precursor lesions have advanced our knowledge on the molecular events occurring during the neoplastic progression in these lesions, providing additional support for distinct molecular pathways involved in tumorigenesis of this subset of CRC [7–10]. Recent gene expression analysis of serrated and conventional colorectal carcinomas has also suggested that CRCs developing through the serrated pathway may require different chemotherapy treatment regimes [11–13]. This is further supported by recent studies that demonstrated colorectal adenocarcinomas characterized by the *BRAF V600E* mutation have significantly worse overall survival when compared to *BRAF wild-type* or *KRAS* mutated adenocarcinomas [3,14–16]. Additionally, SSA/Ps have been reported to be of higher risk of progression [17,18].

Our study attempted the further investigation of underlying molecular alterations in serrated colorectal polyps through gene expression profiling. In validation studies, we employed quantitative reverse transcription–polymerase chain reaction (qRT-PCR) and routine immunohistochemical techniques available in most pathology laboratories using samples from surgical resections and polypectomies. We have identified claudin-1 (CLDN1) as significantly upregulated in polyps bearing the *BRAF V600E* somatic mutation both on a gene expression level and a protein level, regardless of polyp type. Our results indicate that CLDN1 up-regulation occurs early in the development of SSA/P and its overexpression in a proportion of MVHP suggests a close relation between these two lesions of the serrated pathway.

Materials and Methods

Patients and Polyp Samples

Polyp samples used in microarray gene expression profiling and qRT-PCR were obtained from surgical resection specimens. The fresh resection specimens were examined and sampled in a hospital immediately after resection or in the pathology laboratory within 30 minutes of resection. Each polyp was divided into equal portions. Portions were either immediately snap-frozen in liquid nitrogen or formalin fixed and paraffin embedded (FFPE). The frozen sections selected for the study were further verified histologically before analysis.

The diagnostic criteria for SSA/P and MVHP are based on published criteria relying mainly on polyp architecture [9]. The architectural features assessed included crypt branching, horizontal dilatation of basal crypt compartments, and presence of serration at the base of the crypts. Polyps were classified as SSA/P when at least two of these features were present, and only lesions with a sessile configuration and a diameter of 10 mm or more from the right colon (up to the splenic flexure) were classified as SSA/P; MVHP were obtained from the left colon and were <5 mm in diameter. None of the polyps used in microarray gene profiling or RT-PCR contained pericryptal stromal spindle cells, had a conventional adenoma component, or had dysplasia. In addition to morphology, polyps were also characterized by *BRAF* and *KRAS* mutation analyses. No polyps that carried both the *BRAF* and *KRAS* mutations were identified.

Informed consent was obtained from patients before the use of their samples, and the study was approved by the Royal Adelaide Ethics Committee (RAH Protocol No. 001201).

KRAS and BRAF Mutation Screening

DNA was prepared from polyp tissue macro-dissected from FFPE slides using the QIAamp DNA FFPE Tissue Kit (Qiagen, Valencia, CA). Screening for mutations in codons 12 and 13 of the *KRAS* gene was performed using a multiplex assay as described by Di Fiore et al. [19]. The *V600E* mutation in the *BRAF* gene was detected using a single nucleotide primer extension assay comparable to the *KRAS* assay. The portion of exon 15 of the *BRAF* gene encompassing the *V600E* mutation was amplified, and the *V600E* mutation was detected using a SNaPshot Multiplex Kit (Applied Biosystems, Foster City, CA) and a specific primer (C_5TGATTTTGGTCTAGCTACAG). All reactions were run on a 3730 capillary sequencer (Applied Biosystems), and results were analyzed using GeneMapper software version 4.0 (Applied Biosystems).

Microarray Analysis

Frozen samples were sectioned at 6 µm using a cryostat (−25°C) and were immediately stored at −80°C. Before use, the slides were fixed with ice-cold 100% methanol for 10 minutes and then washed with Diethylpyrocarbonate-treated water on ice for 30 seconds and stained with RNase-free hematoxylin solution (Sigma-Aldrich, St Louis, MO) for 1 minute. Finally, the slides were dehydrated with 100% ethanol for 30 seconds and air-dried.

The stained slides were placed onto a PALM Laser Capture dissecting microscope (Zeiss, Oberkochen, Germany). The serrated crypt epithelium of the polyp was catapulted and captured into 50 µl of lysis/binding buffer (Qiagen) using ultraviolet laser cutting according to the manufacturer's recommended protocol. The captured cells were centrifuged, vortexed, and stored at −80°C until RNA isolation. Total RNA was prepared, including column DNase digestion, using the QIAGEN RNeasyPlus Mini Kit (Qiagen). The RNA integrity and concentration for each sample were assessed using the Agilent BioAnalyzer. Only those samples with RNA integrity greater than 5 were used for analysis.

Human Gene 1.0ST arrays (Affymetrix Inc, Santa Clara, CA) were used for gene expression analysis. Extracted RNA from each tissue sample was amplified, fragmented, and biotinylated before hybridization to individual arrays. The hybridized arrays were then loaded onto the Affymetrix Gene Chip Fluidics 450 station, washed, and then stained with a fluorescently labeled antibody. Arrays were scanned using a high-resolution scanner (Affymetrix 3000 7G) by the Adelaide Microarray Centre (Adelaide, Australia).

Statistical Analysis of Microarray Data

Analysis of microarray data was performed using the Partek Genomics Suite (v 6.6; Partek Inc, St Louis, MO). Raw data files were imported using robust multichip averaging background correction, quantile normalization, and median polish probe set summarization. Raw intensity values were adjusted for base-pair (GC) content and probe-specific effects. Differential gene expression was assessed by analysis of variance using the multiple test correction to control for false discovery rate [20]. Gene expression changes between polyp types were considered significant when adjusted P values were less than .05. Ingenuity Pathway Analysis (Ingenuity Systems, Inc, Redwood City, CA) was used to identify potential relationships between differentially expressed genes.

qRT-PCR of CLDN1

RNA was isolated, and its integrity was assessed as for the microarray study. In addition, normal colonic mucosa samples ($n = 10$) obtained from colorectal resections for non-neoplastic conditions were used for the preparation of a pooled, normal reference RNA. The samples were collected, processed, and histologically verified in a similar manner to the polyp tissues.

RNA (10 ng) was converted to cDNA using the iScript cDNA Synthesis Kit (Bio-Rad, Hercules, CA) as per the manufacturer's instructions using the iQ5 Bio-Rad real-time instrument. Briefly, a 20 μl reaction (containing 5 μl of reaction mixture, 10 ng of RNA, and 5 μl of nuclease-free water) was cycled as follows: 5 minutes at 25°C, and then 30 minutes at 42°C, 5 minutes at 85°C, cooled to 4°C, and then again heated to 85°C for 5 minutes.

qRT-PCRs were carried out in triplicate using the iQ SYBR GREEN Supermix (Bio-Rad) according to the manufacturer's instructions. Briefly, a 20 μl reaction (containing 10 μl of iQ SYBR GREEN Supermix, 200 nM each of forward and reverse primers, 2 μl of cDNA template, and nuclease-free water) was cycled on the iQ5 Bio-Rad real-time instrument as follows: 95°C for 3 minutes, then 40 cycles of 95°C for 15 seconds, 58°C for 30 seconds, and 72°C for 30 seconds.

To avoid amplification of genomic DNA, primers were designed to span across two exons. Primers were optimized, and a melt curve analysis was performed to ensure specificity. The cycle threshold value was used to calculate the normalized expression of the selected genes for each sample using the software provided with the iQ5 Bio-Rad real-time instrument. The following primer pairs were used: Glyceraldehyde 3-phosphate dehydrogenase (GAPDH) (as a control gene) forward primer, 5′CAAGGCTGTGGGCAAGGT3′ and reverse primer, 5′GGAAGGCCATGCCAGTGA3′; CLDN-1 forward primer, 5′CTGCCCCAGTGGAGGATTTA3′ and reverse primer, 5′GACATCCACAGCCCCTCGTA3′.

Immunohistochemical Analysis of CLDN1

Sections (4 μm) of paraffin wax–embedded tissue were mounted on coated slides, dewaxed, and rehydrated using standard techniques. Pressure cooker antigen retrieval was performed in 10 mM citrate buffer (pH 6) for 20 minutes. After cooling to 30°C, the sections were incubated for 60 minutes at room temperature with primary CLDN1 monoclonal antibody (1:2500 dilution; Zytomed Systems GmbH, Berlin Germany). The polymer system ADVANCE HRP (Dako Australia Pty Ltd, Victoria, Australia) employing DAB as the detection system was used. Counterstaining was performed using Mayer's hematoxylin. Samples were scored as positive if staining was detected in any of the polyp crypts and negative if there was no staining present. A negative control was performed by omitting the primary antibody.

Statistical Analysis

Statistical analyses were performed using GraphPad Prism (v5.0; GraphPad Software Inc, La Jolla, CA). For qRT-PCR, the Mann-Whitney U test was employed to determine if CLDN1 mRNA expression differed between polyp types. For immunohistochemical analysis, the chi-squared test was used to determine if the differences in CLDN1 staining between each polyp type was statistically significant.

Results

Gene expression analysis was performed on SSA/P ($n = 5$) and MVHP ($n = 5$) samples using Affymetrix Human Gene 1.0ST arrays. The SSA/P samples were obtained from three males and two females (average age 79 years, range 75-82 years). All five polyps were positive for BRAF V600E mutation. Among the MVHP samples, two polyps were positive for KRAS mutation in codon 12 or 13 and the remaining three lesions were wild-type for both BRAF and KRAS. All MVHP samples were obtained from male subjects (average age 62 years, range 24-79 years).

Analysis of variance of gene expression profiles indicated that 744 genes were differentially expressed between SSA/P and MVHP samples (adjusted $P < .05$, fold change ≥ ±2). Furthermore, cluster analysis (hierarchical analysis and principle component analysis) revealed that there was no overlap in the transcriptional profiles of these polyp types, indicating that SSA/P and MVHP have distinct molecular profiles (Figures 1 and W1). The list of differentially expressed genes is shown in Table W1. Bioinformatic network analysis of differentially expressed genes (Ingenuity Pathway Analysis) identified four potential genes as being upstream regulators, i.e., genes that regulate the expression of other genes (either upregulate or downregulate) in a manner consistent with published findings. These upstream regulators include *fibrillin-1, SAM pointed domain containing ETS transcription factor, WNT1 inducible signaling pathway protein 2,* and *synovial apoptosis inhibitor 1*. Each of these genes were predicted to be activated (z-score > 2) on the basis of the direction of the fold change of their downstream targets. The network representing the regulation of expression of these downstream targets is shown in Figure W2.

Statistical and bioinformatic analyses of the gene expression data identified CLDN1 as the most significant differentially expressed gene (based on adjusted P value) and also as a downstream target of WNT1 inducible signaling pathway protein 2 (Figure W2). The expression of CLDN1 was found to be 9.5-fold upregulated in SSA/P samples when compared with MVHP ($P = .003$). Accordingly, we undertook further analysis of this gene in a larger cohort of patient samples to determine its possible use as a marker of the serrated pathway.

qRT-PCR Validation of CLDN1

qRT-PCR was used to investigate CLDN1 expression changes in SSA/P ($n = 18$) and MVHP ($n = 11$) samples with values normalized to GAPDH. Of the 18 SSA/P samples, 10 were males (average age 76 years, range 66-82 years) and 8 were females (average age 74 years,
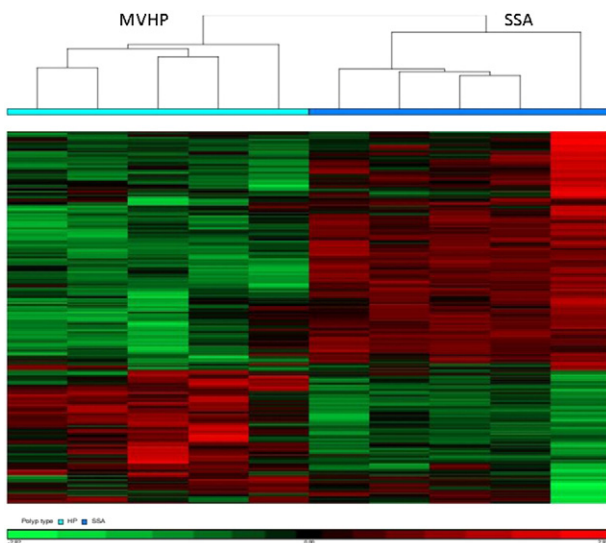
Figure 1. Heat map of the differentially expressed genes between MVHPs and SSA/Ps. The heat map is a representation of statistically significant (adjusted $P < .05$) differentially expressed genes with fold change greater than ± 2 (i.e., 744 genes) between SSA/Ps ($n = 5$, *BRAF* mutant) and MVHPs ($n = 5$, *BRAF* wild type). Hierarchical clustering analysis indicates that SSA/Ps and MVHPs have distinct gene expression patterns. Green indicates decreased expression, and red indicates increased expression.

range 65-82 years). Of the MVHP samples, eight were males (average age 72 years, range 54-78 years) and three were females (average age 54 years, range 49-56 years). Of the SSA/P group, 15 were positive for *BRAF V600E* mutation (9 males, average age 74 years; 6 females, average age 68 years), 1 was positive for *KRAS mutation* (female, age 75 years), and 2 were wild-type for both the *KRAS* and *BRAF* genes (1 male, age 82 years; 1 female, age 79 years). Of the MVHP group, six were positive for *BRAF V600E* mutation (four males; average age 70 years; two females, average age 52 years), three were positive for *KRAS* mutation (two males, average age 72 years; one female, age 56 years), and two samples were wild-type for both the *KRAS* and *BRAF* genes (two males, average age 73 years).

A nonparametric approach (Mann-Whitney *U* test) was employed to determine if *CLDN1* expression was statistically different between the two polyp groups. When based on morphologic classification alone, *CLDN1* expression was significantly upregulated in SSA/P ($n = 18$) when compared to MVHP ($n = 11$) ($P < .0001$; Figure 2A). When these polyps were classified according to *BRAF V600E* mutation status, CLDN1 expression was significantly elevated in *BRAF V600E* mutant polyps ($n = 23$) when compared to those with no mutation ($n = 6$; $P < .0005$; Figure 2B).

Immunohistochemical Analysis of CLDN1 Expression

Serrated polyps displaying the morphology of traditional MVHP were found to be a heterogeneous group differing in an underlying gene mutation and also in the mRNA expression of *CLDN1* (Figure 2). Hence, for immunohistochemical analysis, samples ($n = 222$) were divided into four groups: SSA/P (characterized by *BRAF V600E* mutation, $n = 53$), MVHP with the *BRAF V600E* mutation ($n = 111$), MVHP with mutations in codon 12 or 13 of the *KRAS* gene ($n = 23$), and MVHP without mutation in either the *BRAF* or *KRAS* gene ($n = 35$). Specific patient and polyp characteristics are summarized in Table 1.

Representative CLDN1 immunostaining in SSA/P that is either BRAF V600E mutant or wild-type is shown in Figure 3. Analysis of these immunohistochemical data showed that the majority of *BRAF V600E* mutant SSA/P and MVHP were positive for CLDN1 expression (89% and 81%, respectively). This is in contrast to MVHP with *KRAS* mutations where only 35% were found to be positive for CLDN1 expression (Table 2). Furthermore, in those MVHP where no mutation was detected in either the *KRAS* or *BRAF* gene, 54% of these were positive for CLDN1 expression. Further
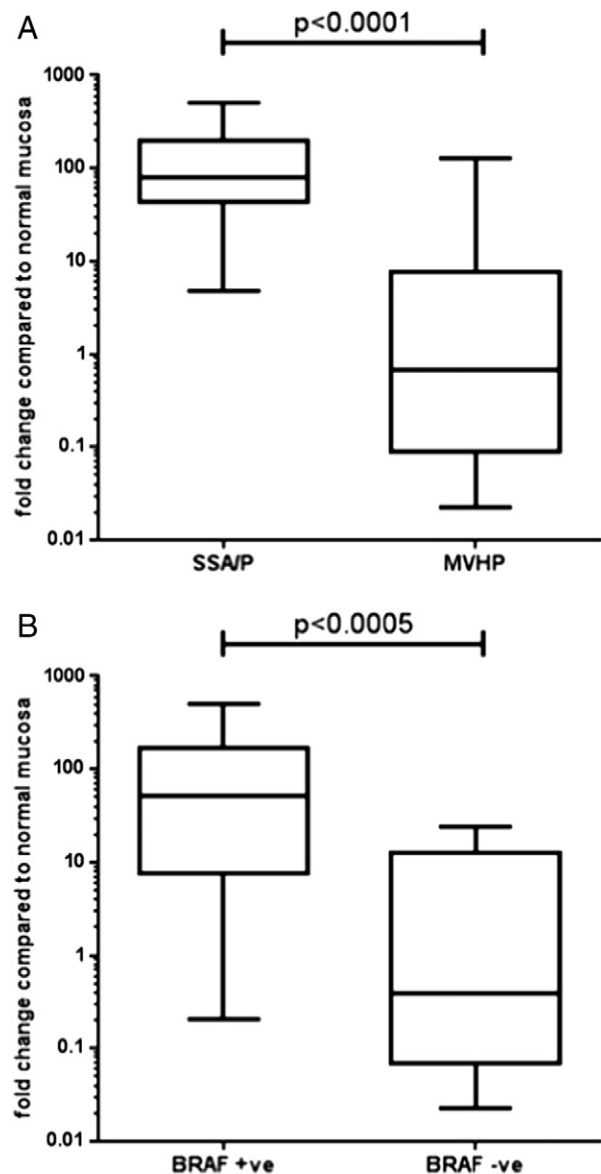
Figure 2. Expression levels of *CLDN1* by qRT-PCR. (A) Expression levels of *CLDN1* in SSA/P and MVHPs based on morphology compared to normal colonic mucosal tissue (mean value of 1). The median expression levels for *CLDN1* was significantly upregulated in SSA/P ($n = 18$) when compared to MVHPs ($n = 11$; $P = 0.0001$). (B) Expression levels of *CLDN1* in polyps stratified by BRAF mutation status. *CLDN1* expression was significantly ($P < .0005$) elevated in polyps positive for the *BRAF V600E* mutation ($n = 23$) when compared to polyps where the mutation was not detected ($n = 6$). Abbreviations: *BRAF* +ve, *BRAF V600E* mutant; *BRAF* −ve, *BRAF* wild type.

Table 1. Characteristics of the Patient Cohort and Precursor Lesions Used for Immunohistochemical Analysis of CLDN1 Expression

	SSA/P (n = 53)	MVHP (n = 169)		
Patient cohort				
Female (average age)	22 (63 years)	44 (55 years)	8 (65 years)	15 (60 years)
Male (average age)	31 (60 years)	66 (60 years)	15 (62 years)	20 (55 years)
Tumor location				
Right colon	29	5	2	2
Left colon	21	77	14	24
Not recorded	3	29	7	9
Mutation status				
BRAF mutant	53	111		
KRAS mutant			23	
No mutation in KRAS or BRAF				35

Abbreviations: BRAF mutant, positive for V600E mutation; KRAS mutant, positive for mutation in codon 12 or 13.

analysis (chi-squared test) determined that positive CLDN1 expression was significantly associated with *BRAF V600E* mutation independently of polyp morphology (Table 3). Negative controls showed no staining.

Discussion

The concept of hyperplastic polyps being associated with CRC was raised three decades ago [21] and despite anecdotal case reports describing CRCs arising in giant hyperplastic polyps or in the background of multiple hyperplastic polyps, the idea has remained unchallenged for many years. Since then, a variant of the hyperplastic polyp, the SSA/P, has been implicated in CRC development and subsequently accepted as a precursor lesion of predominantly right-sided CRC with supportive molecular evidence initially reported by Jass et al. [22]. Detailed characterization of serrated colorectal polyps subdivided the group of hyperplastic polyps into three categories: microvesicular, goblet cell rich, and mucin poor, with the micro-vesicular type being the most prevalent [3]. MVHP and SSA/P have overlapping morphologic features and distinction between these polyp types in routine practice may be difficult or impossible, particularly when the polyps are small or when dealing with biopsies rather than excised lesions. While SSA/Ps are well known to harbor the somatic *BRAF V600E* mutation, this molecular alteration is also present in a significant proportion of MVHPs [23–26] The presence of overlapping morphology with SSA/P and molecular alterations, including the somatic *BRAF V600E* mutation, raised the possibility of MVHP to have the ability to progress to more advanced lesions of the serrated pathway [25,27,2].

In addition to mutations in the *BRAF* gene, lesions of the serrated pathway are also characterized by high frequency of MSI and CIMP [28–30]. Our gene expression analysis has identified 744 genes that were differentially expressed between MVHP and SSA/P stratified by *BRAF V600E* mutation status (adjusted $P < .05$, fold change $\geq \pm 2$), providing convincing evidence that these polyp types are most likely derived from distinct molecular pathways, which is consistent with other published reports [9,11–13,31]. Several studies have attempted to identify biomarkers of SSA/P to develop a diagnostic tool to assist the pathologist to correctly diagnose this polyp type or to expand our knowledge on biology and underlying molecular events involved in malignant transformation of these lesions [8–10]. A recently published study that employed microarray gene expression profiling with RT-PCR validation on a similar number of MVHPs and SSA/Ps revealed a strong association of the *annexin A10* gene with SSA/P but not with MVHP making it a potential biomarker of SSA/P [10].

Mapping of the most differentially expressed genes in the same study onto 12 core cancer signaling pathways demonstrated a significant up-regulation of the *CLDN1* gene in SSA/P. Interestingly, both genes were in the top six of the most differentially expressed genes in our study (sixth and first, respectively). The fact that *CLDN1* was found to be upregulated in SSA/P in our microarray and not in the previous work may reflect the stratification of our polyps based on *BRAF* mutation status and/or sampling differences as our samples were obtained with assistance of a laser capture microscope.

Interestingly, the same study demonstrated overexpression of a trefoil factor family gene, *TFF2*, in SSA/P and not in MVHP. These results and our previous observation of overexpression of the *TFF1* gene in SSAs indicate the likely involvement of *trefoil factor family* genes in serrated pathway neoplasia [9]. A recently published investigation of immunohistochemical detection of claudin-18 protein (like CLDN1, a component of tight junctions) in serrated pathway lesions demonstrated a higher expression of this protein in SSA/P than in hyperplastic polyps or conventional adenomas [8].

In CRC, reports of CLDN1 expression have been contradictory. For example, overexpression of CLDN1 in adenocarcinoma tissue in comparison to normal mucosa has been reported [32–34], and more recently, Bezdekova et al. demonstrated elevated CLDN1 expression in a cohort of 42 adenomas relative to normal epithelium [35]. In these studies, cytoplasmic CLDN1 was correlated with disease progression. However, low CLDN1 tumor expression has also been observed and a link between metastasis and poor patient prognosis has been proposed [36–38]. These studies, however, did not report on molecular characterization of the patient samples tested, and it is possible that these opposing results can be explained by molecular features such as *BRAF* mutation status, MSI, or CIMP. Further studies on our patient cohort exploring the association between mutations in the *BRAF* gene, CLDN1 staining, and patient outcome are warranted to better understand their use for prognosis.

The dysregulation of CLDN1 expression has also been postulated as a contributor to colon cancer progression and its up-regulation has been shown to be associated with the disorganization of tight junction fibrils, leading to an increase in paracellular permeability [32]. CLDN1 expressing xenograft tumors have been demonstrated to have increased potential for invasion and metastatic behaviour [39]. In addition, a positive correlation of CLDN1 expressing CRC cells and their resistance to anoikis also suggests that CLDN1 may influence tumor growth and evolution [40]. The role of CLDN1 in the progression of SSA to cancer has not been investigated and is unknown. However, the evolution of serrated lesions to CRC appears to be accelerated and faster than conventional adenomas [18,41] and may be related to resistance to anoikis and cellular discohesion. As CLDN1 is associated with both processes, the serrated polyps showing CLDN1 overexpression may have increased potential for progression to higher grade lesions through the serrated pathway neoplasia.

In gastric epithelial cells, CLDN1 has also been described as a target of the RUNX3 transcription factor [42]. In intestinal tumors, RUNX3 can potentially inactivate Wnt signaling by interacting with the β-catenin/TCF4 complex [43]. *RUNX3* is one of the core genes used to classify CIMP high CRC [5] and it is possible that in this subset of tumors, promoter hypermethylation and subsequent loss of RUNX3 expression can attenuate β-catenin/TCF signaling leading to elevated CLDN1 expression. Activation of Wnt signaling in SSA/P is controversial with evidence in the literature to both support and oppose this hypothesis. Abnormal β-catenin staining has been shown
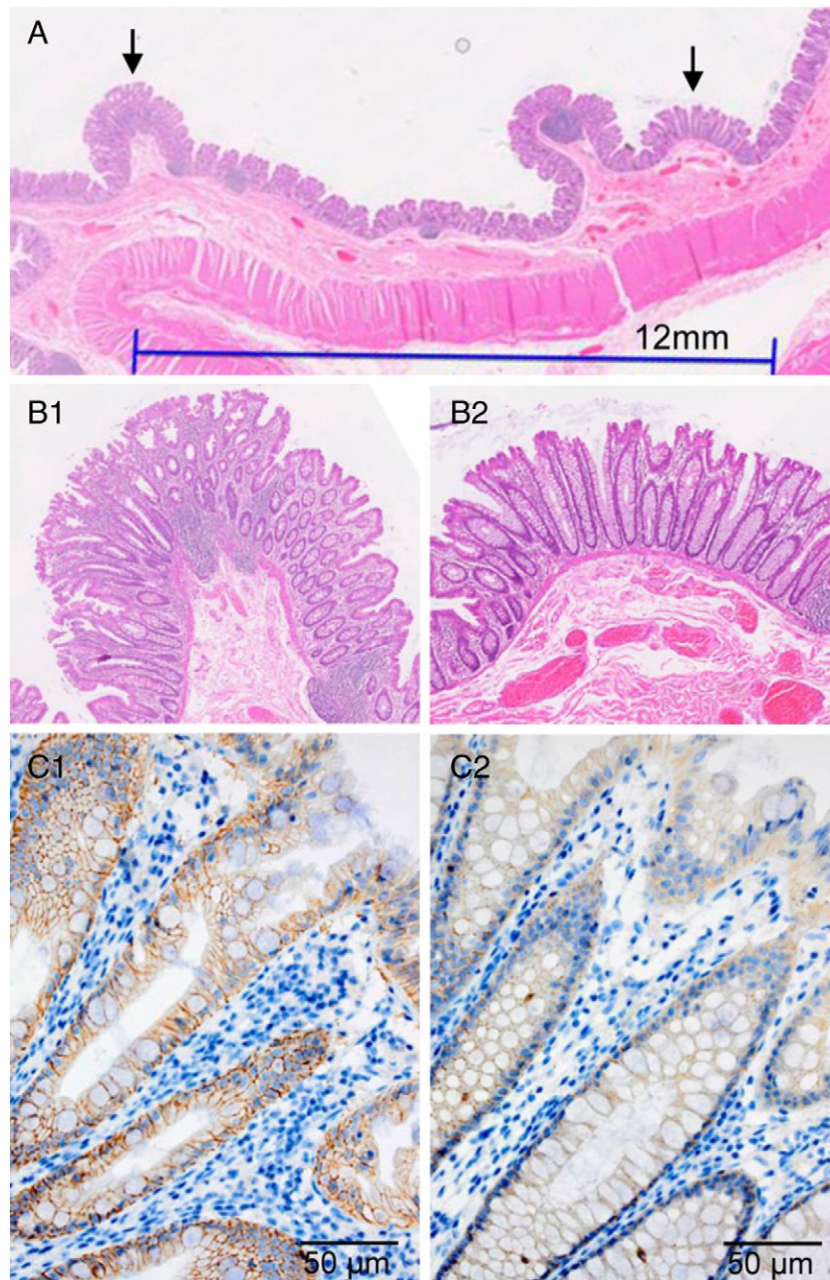
Figure 3. Representative immunostaining of CLDN1 protein in SSA/Ps. Two small serrated, non-dysplastic polyps measuring less than 2 mm, located 12 mm apart in rectosigmoid resection specimen are indicated by arrows (A; hematoxylin and eosin stain). The polyp on the left side (B1; hematoxylin and eosin stain) had a *BRAF V600* somatic mutation and demonstrates a strong membranous expression of CLDN1 on immunohistochemistry (C1; original magnification, × 100). The diminutive polyp on the right side harbored *KRAS* mutation in codon 12 and showed no staining for CLDN1 on immunohistochemistry (C2; original magnification, × 100).

Table 2. CLDN1 Immunostaining in SSA/Ps and MVHPs with *BRAF* and *KRAS* Gene Mutation Status

	Positive CLDN1 staining	Negative CLDN1 staining
SSA/P, *BRAF* mutant (n = 53)	47 (89%)	6 (11%)
MVHP, *BRAF* mutant (n = 111)	90 (81%)	21 (19%)
MVHP, *KRAS* mutant (n = 23)	8 (35%)	15 (65%)
MVHP, no mutation (n = 35)	19 (54%)	16 (48%)

Abbreviations: *BRAF* mutant, positive for *V600E* mutation; *KRAS* mutant, positive for mutation in codon 12 or 13.

in a subset of SSA/P, and Yachida et al. have reported an association between nuclear β-catenin staining and *BRAF V600E* mutation [44–46]). In contrast, other studies have demonstrated the opposite or involvement of Wnt signaling only in SSA with neoplastic progression, implying that Wnt signaling may only be activated late in the progression of disease for SSA/P [47,48].

Interestingly, CLDN1 is expressed in recently described perineural-like stromal proliferations in a small fraction of serrated colorectal polyps including MVHP and SSA/P [49]. These stromal pericryptal

Table 3. Relationship between Positive CLDN1 Immunostaining and *BRAF* and *KRAS* Gene Mutation Status

	SSA/P	MVHP		
	BRAF Mutant	*BRAF* Mutant	*KRAS* Mutant	No Mutation
SSA/P, *BRAF* mutant (n = 53)	N/A	$P = .2246$	$P < .0001$	$P = .0006$
MVHP, BRAF mutant (n = 111)	$P = .2246$	N/A	$P < .0001$	$P = .0021$
MVHP, KRAS mutant (n = 23)	$P < .0001$	$P < .0001$	N/A	$P = .1484$
MVHP, no mutation (n = 53)	$P = .0006$	$P = .0021$	$P = .1485$	N/A

Abbreviations: *BRAF* mutant, positive for *V600E* mutation; *KRAS* mutant, positive for mutation in codon 12 or 13; N/A, statistical comparison not applicable.

proliferations are usually focal and not exceeding 10% of polyp tissue; however, in rare cases, the spindle cells extensively populate the lamina propria to become a dominant cell population of the polyp. Previously reported colorectal lesions such as intestinal perineuriomas [50] and fibroblastic polyps [51] are most certainly exaggerated examples of these stromal proliferations and widen the spectrum of serrated colorectal polyps as the vast majority of these have the somatic *BRAF V600E* mutation [16].

This is the first report describing a strong correlation between CLDN1 expression and *BRAF V600E* mutation status in serrated colorectal polyps. *CLDN1* mRNA and protein expression was found to be significantly elevated in SSA/P and MVHP with *BRAF V600E* mutation. To date, there is no established direct link between the oncogenic and activating *BRAF V600E* mutation and regulation of CLDN1 expression. Our results support the view of a close relationship between *BRAF* mutated MVHP and SSA/P, which may, in fact, represent a continuous spectrum of the same neoplastic process [27]. Precise subclassification of MVHP may require the use of additional ancillary techniques including CLDN1 immunohistochemistry to identify the lesions with different biologic potential for neoplastic progression to more advanced serrated pathway lesions.

Supplementary data to this article can be found online at http://dx.doi.org/10.1016/j.neo.2014.05.008.

Author's contributions

MC participated in study design, microarray analysis, performed RT-PCR and participated in data analysis and drafting manuscript. KYCF participated in data analysis and drafting of manuscript. JM participated in study design and patient selection, GVB participated in RT PCR, LJC contributed to study design and drafting manuscript, MT contributed to patient selection and data analysis, GC performed mutational analysis of *BRAF* and *KRAS*, EB and LF participated in selection of polyp samples and immunohistochemistry scoring, TT and HT performed immunohistochemistry staining and DNA extraction. AR participated in study design, pathological examination of polyp samples and drafting of the manuscript. All authors read and approved manuscript.

Acknowledgments

References

[1] Vogelstein B, Fearon ER, Hamilton SR, Kern SE, Preisinger AC, Leppert M, Nakamura Y, White R, Smits AM, and Bos JL (1988). Genetic alterations during colorectal-tumor development. *N Engl J Med* **319**, 525–532.

[2] Rex DK, Ahnen DJ, Baron JA, Batts KP, Burke CA, Burt RW, Goldblum JR, Guillem JG, Kahi CJ, and Kalady MF, et al (2012). Serrated lesions of the colorectum: review and recommendations from an expert panel. *Am J Gastroenterol* **107**, 1315–1329 [quiz 1314, 1330].

[3] Torlakovic E, Skovlund E, Snover DC, Torlakovic G, and Nesland JM (2003). Morphologic reappraisal of serrated colorectal polyps. *Am J Surg Pathol* **27**, 65–81.

[4] Bettington M, Walker N, Clouston A, Brown I, Leggett B, and Whitehall V (2013). The serrated pathway to colorectal carcinoma: current concepts and challenges. *Histopathology* **62**, 367–386.

[5] Weisenberger DJ, Siegmund KD, Campan M, Young J, Long TI, Faasse MA, Kang GH, Widschwendter M, Weener D, and Buchanan D, et al (2006). CpG island methylator phenotype underlies sporadic microsatellite instability and is tightly associated with BRAF mutation in colorectal cancer. *Nat Genet* **38**, 787–793.

[6] Fearon ER and Vogelstein B (1990). A genetic model for colorectal tumorigenesis. *Cell* **61**, 759–767.

[7] Burnett-Hartman AN, Newcomb PA, Potter JD, Passarelli MN, Phipps AI, Wurscher MA, Grady WM, Zhu LC, Upton MP, and Makar KW (2013). Genomic aberrations occurring in subsets of serrated colorectal lesions but not conventional adenomas. *Cancer Res* **73**, 2863–2872.

[8] Sentani K, Sakamoto N, Shimamoto F, Anami K, Oue N, and Yasui W (2013). Expression of olfactomedin 4 and claudin-18 in serrated neoplasia of the colorectum: a characteristic pattern is associated with sessile serrated lesion. *Histopathology* **62**, 1018–1027.

[9] Caruso M, Moore J, Goodall GJ, Thomas M, Phillis S, Tyskin A, Cheetham G, Lerda N, Takahashi H, and Ruszkiewicz A (2009). Over-expression of cathepsin E and trefoil factor 1 in sessile serrated adenomas of the colorectum identified by gene expression analysis. *Virchows Arch* **454**, 291–302.

[10] Gonzalo DH, Lai KK, Shadrach B, Goldblum JR, Bennett AE, Downs-Kelly E, Liu X, Henricks W, Patil DT, and Carver P, et al (2013). Gene expression profiling of serrated polyps identifies annexin A10 as a marker of a sessile serrated adenoma/polyp. *J Pathol* **230**, 420–429.

[11] Conesa-Zamora P, García-Solano J, García-García F, Turpin Mdel C, Trujillo-Santos J, Torres-Moreno D, Oviedo-Ramírez I, Carbonell-Muñoz R, Muñoz-Delgado E, and Rodriguez-Braun E, et al (2013). Expression profiling shows differential molecular pathways and provides potential new diagnostic biomarkers for colorectal serrated adenocarcinoma. *Int J Cancer* **132**, 297–307.

[12] Joyce T, Oikonomou E, Kosmidou V, Makrodouli E, Bantounas I, Avlonitis S, Zografos G, and Pintzas A (2012). A molecular signature for oncogenic BRAF in human colon cancer cells is revealed by microarray analysis. *Curr Cancer Drug Targets* **12**, 873–898.

[13] Laiho P, Kokko A, Vanharanta S, Salovaara R, Sammalkorpi H, Jarvinen H, Mecklin JP, Karttunen TJ, Tuppurainen K, and Davalos V, et al (2007). Serrated carcinomas form a subclass of colorectal cancer with distinct molecular basis. *Oncogene* **26**, 312–320.

[14] El-Osta H, Falchook G, Tsimberidou A, Hong D, Naing A, Kim K, Wen S, Janku F, and Kurzrock R (2011). BRAF mutations in advanced cancers: clinical characteristics and outcomes. *PLoS One* **6**, e25806.

[15] Kalady MF, Dejulius KL, Sanchez JA, Jarrar A, Liu X, Manilich E, Skacel M, and Church JM (2012). BRAF mutations in colorectal cancer are associated with distinct clinical characteristics and worse prognosis. *Dis Colon Rectum* **55**, 128–133.

[16] Pai RK, Jayachandran P, Koong AC, Chang DT, Kwok S, Ma L, Arber DA, Balise RR, Tubbs RR, and Shadrach B, et al (2012). BRAF-mutated, microsatellite-stable adenocarcinoma of the proximal colon: an aggressive adenocarcinoma with poor survival, mucinous differentiation, and adverse morphologic features. *Am J Surg Pathol* **36**, 744–752.

[17] Goldstein NS (2006). Small colonic microsatellite unstable adenocarcinomas and high-grade epithelial dysplasias in sessile serrated adenoma polypectomy specimens: a study of eight cases. *Am J Clin Pathol* **125**, 132–145.

[18] Oono Y, Fu K, Nakamura H, Iriguchi Y, Yamamura A, Tomino Y, Oda J, Mizutani M, Takayanagi S, and Kishi D, et al (2009). Progression of a sessile serrated adenoma to an early invasive cancer within 8 months. *Dig Dis Sci* **54**, 906–909.

[19] Di Fiore F, Blanchard F, Charbonnier F, Le Pessot F, Lamy A, Galais MP, Bastit L, Killian A, Sesboue R, and Tuech JJ, et al (2007). Clinical relevance of KRAS mutation detection in metastatic colorectal cancer treated by Cetuximab plus chemotherapy. *Br J Cancer* **96**, 1166–1169.

[20] Benjamini Y and Hochberg Y (1995). Controlling the false discovery rate: A practical and powerful approach to multiple testing. *J R Stat Soc B* **57**, 289–300.

[21] Jass JR (1983). Relation between metaplastic polyp and carcinoma of the colorectum. *Lancet* **1**, 28–30.

[22] Jass JR, Iino H, Ruszkiewicz A, Painter D, Solomon MJ, Koorey DJ, Cohn D, Furlong KL, Walsh MD, and Palazzo J, et al (2000). Neoplastic progression occurs through mutator pathways in hyperplastic polyposis of the colorectum. *Gut* **47**, 43–49.

[23] Chan TL, Zhao W, Leung SY, and Yuen ST (2003). BRAF and KRAS mutations in colorectal hyperplastic polyps and serrated adenomas. *Cancer Res* **63**, 4878–4881.

[24] Kambara T, Simms LA, Whitehall VL, Spring KJ, Wynter CV, Walsh MD, Barker MA, Arnold S, McGivern A, and Matsubara N, et al (2004). BRAF mutation is associated with DNA methylation in serrated polyps and cancers of the colorectum. *Gut* **53**, 1137–1144.

[25] Kim KM, Lee EJ, Kim YH, Chang DK, and Odze RD (2010). KRAS mutations in traditional serrated adenomas from Korea herald an aggressive phenotype. *Am J Surg Pathol* **34**, 667–675.

[26] Yang S, Farraye FA, Mack C, Posnik O, and O'Brien MJ (2004). BRAF and KRAS Mutations in hyperplastic polyps and serrated adenomas of the colorectum: relationship to histology and CpG island methylation status. *Am J Surg Pathol* **28**, 1452–1459.

[27] Mesteri I, Bayer G, Meyer J, Capper D, Schoppmann SF, von Deimling A, and Birner P (2014). Improved molecular classification of serrated lesions of the colon by immunohistochemical detection of *BRAF V600E. Mod Pathol* **27**, 135–144.

[28] Iino H, Jass JR, Simms LA, Young J, Leggett B, Ajioka Y, and Watanabe H (1999). DNA microsatellite instability in hyperplastic polyps, serrated adenomas, and mixed polyps: a mild mutator pathway for colorectal cancer? *J Clin Pathol* **52**, 5–9.

[29] Issa JP (2004). CpG island methylator phenotype in cancer. *Nat Rev Cancer* **4**, 988–993.

[30] O'Brien MJ, Yang S, Clebanoff JL, Mulcahy E, Farraye FA, Amorosino M, and Swan N (2004). Hyperplastic (serrated) polyps of the colorectum: relationship of CpG island methylator phenotype and K-ras mutation to location and histologic subtype. *Am J Surg Pathol* **28**, 423–434.

[31] Garcia-Solano J, Conesa-Zamora P, Carbonell P, Trujillo-Santos J, Torres-Moreno DD, Pagan-Gomez I, Rodriguez-Braun E, and Perez-Guillermo M (2012). Colorectal serrated adenocarcinoma shows a different profile of oncogene mutations, MSI status and DNA repair protein expression compared to conventional and sporadic MSI-H carcinomas. *Int J Cancer* **131**, 1790–1799.

[32] de Oliveira SS, de Oliveira IM, De Souza W, and Morgado-Diaz JA (2005). Claudins upregulation in human colorectal cancer. *FEBS Lett* **579**, 6179–6185.

[33] Gröne J, Weber B, Staub E, Heinze M, Klaman I, Pilarsky C, Hermann K, Castanos-Velez E, Röpcke S, and Mann B, et al (2007). Differential expression of genes encoding tight junction proteins in colorectal cancer: frequent dysregulation of claudin-1, -8 and -12. *Int J Colorectal Dis* **22**, 651–659.

[34] Kinugasa T, Huo Q, Higashi D, Shibaguchi H, Kuroki M, Tanaka T, Futami K, Yamashita Y, Hachimine K, and Maekawa S, et al (2007). Selective up-regulation of claudin-1 and claudin-2 in colorectal cancer. *Anticancer Res* **27**, 3729–3734.

[35] Bezdekova M, Brychtova S, Sedlakova E, Langova K, Brychta T, and Belej K (2012). Analysis of snail-1, e-cadherin and claudin-1 expression in colorectal adenomas and carcinomas. *Int J Mol Sci* **13**, 1632–1643.

[36] Ersoz S, Mungan S, Cobanoglu U, Turgutalp H, and Ozoran Y (2011). Prognostic importance of Claudin-1 and Claudin-4 expression in colon carcinomas. *Pathol Res Pract* **207**, 285–289.

[37] Nakagawa S, Miyoshi N, Ishii H, Mimori K, Tanaka F, Sekimoto M, Doki Y, and Mori M (2011). Expression of CLDN1 in colorectal cancer: a novel marker for prognosis. *Int J Oncol* **39**, 791–796.

[38] Resnick MB, Konkin T, Routhier J, Sabo E, and Pricolo VE (2005). Claudin-1 is a strong prognostic indicator in stage II colonic cancer: a tissue microarray study. *Mod Pathol* **18**, 511–518.

[39] Dhawan P, Singh AB, Deane NG, No Y, Shiou SR, Schmidt C, Neff J, Washington MK, and Beauchamp RD (2005). Claudin-1 regulates cellular transformation and metastatic behavior in colon cancer. *J Clin Invest* **115**, 1765–1776.

[40] Singh AB, Sharma A, and Dhawan P (2012). Claudin-1 expression confers resistance to anoikis in colon cancer cells in a Src-dependent manner. *Carcinogenesis* **33**, 2538–2547.

[41] Endo A, Koizumi H, Takahashi M, Tamura T, Tatsunami S, Watanabe Y, and Takagi M (2013). A significant imbalance in mitosis versus apoptosis accelerates the growth rate of sessile serrated adenoma/polyps. *Virchows Arch* **462**, 131–139.

[42] Chang TL, Ito K, Ko TK, Liu Q, Salto-Tellez M, Yeoh KG, Fukamachi H, and Ito Y (2010). Claudin-1 has tumor suppressive activity and is a direct target of RUNX3 in gastric epithelial cells. *Gastroenterology* **138**(255–265), e251–e253.

[43] Ito K, Lim AC, Salto-Tellez M, Motoda L, Osato M, Chuang LS, Lee CW, Voon DC, Koo JK, and Wang H, et al (2008). RUNX3 attenuates β-catenin/T cell factors in intestinal tumorigenesis. *Cancer Cell* **14**, 226–237.

[44] Li L, Fu X, Zhang W, Xiao L, Qiu Y, Peng Y, Shi L, Chen X, Zhou X, and Deng M (2013). Wnt signaling pathway is activated in right colon serrated polyps correlating to specific molecular form of β-catenin. *Hum Pathol* **44**, 1079–1088.

[45] Wu JM, Montgomery EA, and Iacobuzio-Donahue CA (2008). Frequent beta-catenin nuclear labeling in sessile serrated polyps of the colorectum with neoplastic potential. *Am J Clin Pathol* **129**, 416–423.

[46] Yachida S, Mudali S, Martin SA, Montgomery EA, and Iacobuzio-Donahue CA (2009). Beta-catenin nuclear labeling is a common feature of sessile serrated adenomas and correlates with early neoplastic progression after *BRAF* activation. *Am J Surg Pathol* **33**, 1823–1832.

[47] Fu X, Yang X, Chen K, and Zhang Y (2011). Retained cell-cell adhesion in serrated neoplastic pathway as opposed to conventional colorectal adenomas. *J Histochem Cytochem* **59**, 158–166.

[48] Fujita K, Yamamoto H, Matsumoto T, Hirahashi M, Gushima M, Kishimoto J, Nishiyama K, Taguchi T, Yao T, and Oda Y (2011). Sessile serrated adenoma with early neoplastic progression: a clinicopathologic and molecular study. *Am J Surg Pathol* **35**, 295–304.

[49] Pai RK, Mojtahed A, Rouse RV, Soetikno RM, Kaltenbach T, Ma L, Arber DA, Plesec TP, and Goldblum JR (2011). Histologic and molecular analyses of colonic perineurial-like proliferations in serrated polyps: perineurial-like stromal proliferations are seen in sessile serrated adenomas. *Am J Surg Pathol* **35**, 1373–1380.

[50] Hornick JL and Fletcher CD (2005). Intestinal perineuriomas: clinicopathologic definition of a new anatomic subset in a series of 10 cases. *Am J Surg Pathol* **29**, 859–865.

[51] Groisman GM and Polak-Charcon S (2008). Fibroblastic polyp of the colon and colonic perineurioma: 2 names for a single entity? *Am J Surg Pathol* **32**, 1088–1094.